Carbohydrate Polymers 87 (2012) 1460–1466

Contents lists available at SciVerse ScienceDirect

Carbohydrate Polymers

journal homepage: www.elsevier.com/locate/carbpol

Structural and conformational differences of acylated hyaluronan modified in protic and aprotic solvent system

Daniela Šmejkalová [a,*], Martina Hermannová [a], Romana Šuláková [a], Alena Průšová [b], Jiří Kučerík [b], Vladimír Velebný [a]

[a] Contipro C, Dolní Dobrouč 401, 561 02 Dolní Dobrouč, Czech Republic
[b] Brno University of Technology, Faculty of Chemistry, Purkyňova 118, 612 00 Brno, Czech Republic

ARTICLE INFO

Article history:
Received 7 July 2011
Received in revised form 2 September 2011
Accepted 12 September 2011
Available online 29 September 2011

Keywords:
Hyaluronan
Acylation
NMR
DSC
UV–vis
Mass spectrometry

ABSTRACT

Acylated hyaluronan (HA) in aqueous (DMSO/H_2O) and nonaqueous (DMSO) solutions was studied by means of nuclear magnetic resonance, differential scanning calorimetry (DSC), mass spectrometry and UV/vis spectroscopy. It has been demonstrated that structural and conformational properties of the acylated hyaluronan derivates are strongly dependent on the nature of reaction solvent. Acylation in DMSO was more selective than that carried out in DMSO/H_2O, though in both cases in average a maximum of one acyl chain was detected per HA dimer. The hydrophobic functionalization of hyaluronan induced its interaction with hydrophobic dye as a consequence of acyl chain aggregation. The higher the degree of acylation the more hydrophobic dye was interacting with HA. For concentrated samples, aggregation was more evident in case of acylated HA in aqueous solution. This phenomenon was explained by its different conformational arrangement in solution which was further supported by DSC data indicating an existence of hydrophobic cavities. The formation of self-aggregated assemblies indicates potential applications of this type of HA derivate as drug delivery system.

© 2011 Elsevier Ltd. All rights reserved.

1. Introduction

Carbohydrate fatty acid esters are an important class of biodegradable and non-toxic surfactants with broad applications in food, cosmetics and pharmaceutical industries as detergents, oral care products and medical supplies (Hill & LeHen-Ferrenbach, 2008). They were also reported to be applicable as antibiotics and antitumorals (Deleu & Paquot, 2004). In addition, non-toxic and biodegradable polysaccharide surfactants are considered to be attractive drug delivery systems. Among polysaccharides, a great attention is focused on esterification of hyaluronan (HA) (Kawaguchi, Matsukawa, & Ishigami, 1993; Kong, Chen, & Park, 2011; Taglienti, Valentini, Sequi, & Crescenzi, 2005).

HA is a linear polysaccharide consisting of alternating β-1,4-linked units of β-1,3-linked glucuronic acid and *N*-acetyl-D-glucosamine (Laurent, 1998; Scott, 1998). HA is a main component of the extracellular matrix in connective, epithelial, and neural tissues and is known to play an important role in organ development, cell proliferation and migration. Additionally, HA contributes to the lubrication and maintenance of cartilage, where it is a major component of synovial fluid and forms a coating around chondrocytes (Collis et al., 1998; Entwistle, Hall, & Turley, 1996; Laurent, 1998). Except for being biodegradable and non-toxic, HA is biocompatible and renewable, which is important on industrial scale production of HA derivates.

The major advantage of modified HA over the native HA is the higher resistance against enzymatic degradation (Abatangelo, Barbucci, Brun, & Lamponi, 1997; Prestwitch, Marecak, Marecek, Vercuysse, & Ziebell, 1998; Šoltés et al., 2006). In addition, besides retaining its inherently superior properties, HA derivates acquire additional physicochemical characteristics that can be tailored according to the desired requirements. For example, HA having desired amount of hydrophobic functional groups may be achieved varying the degree of substitution. In case of esterification, the degree of substitution and the length of attached carbon chain are directly related to conformational behavior of the substituted molecule in solution and the possibility of forming supramolecular assemblies (Akiyoshi & Sunamoto, 1996). Formation of supramolecular assemblies is than in turn related to the possibility of carbohydrate interaction with non-polar compounds and therefore directly affects its pharmaceutical and industrial applications. Modified HA is therefore also considered to have a great potential as a novel drug carrier in form of conjugates. Despite its excellent biocompatible and biodegradable properties, HA based drug delivery systems have been reported to work as an efficient depot for sustained release of protein drugs without denaturation (Oh et al., 2010; Prestwitch & Vercruysse, 1998). Moreover, the absence of positive charge on HA surface alleviate the problems

* Corresponding author. Tel.: +420 465519569; fax: +420 465543793.
E-mail address: smejkalova@contipro.cz (D. Šmejkalová).

0144-8617/$ – see front matter © 2011 Elsevier Ltd. All rights reserved.
doi:10.1016/j.carbpol.2011.09.057

with severe cytotoxicity and aggregations with serum proteins in the body found for cationic liposomes and polymers investigated as drug carriers (Oh et al., 2010).

In this study, we followed the structural and conformational changes of HA induced after acylation with hexanoic anhydride in DMSO and DMSO/H_2O solvent. The main attention was focused on the comparison of reaction selectivity and conformational changes of HA followed after acylation. The structural changes were studied by NMR, ESI-MS/MS and DSC. Formation of hydrophobic domains was examined by comparing the ability of acyl derivates to dissolve a hydrophobic dye.

2. Experimental

2.1. Materials

Hyaluronic acid sodium salt (200 kDa, 155 kDa and 34 kDa) was provided by CPN Dolní Dobrouč, Czech Republic. Hexanoic anhydrides, triethylamine, dimethylsulfoxide, dimethylaminopyridine (DMAP), Oil Red O (Solvent Red 27, Sudan Red 5B, C.I. 26125, $C_{26}H_{24}N_4O$), and deuterated water were of analytical grade and purchased from Sigma–Aldrich.

2.2. Preparation of hyaluronan acid form and hyaluronan sodium salt

Hyaluronan (M_w = 200 kDa, 15 g) was dissolved in 600 mL of demineralized water and then Amberlite IR 120 Na exchange resin (wet state, 100 g) was added to the mixture. The mixture was kept at room temperature with occasional stirring. Cation exchange resin was removed by centrifugation at 5000 rpm for 5 min and the resulting solution was lyophilized. About 13 g of hyaluronan acid form M_w = 50 kDa was obtained.

Since each transformation of hyaluronan into its acid form causes HA degradation, it was necessary to have a comparable starting M_w of both HA sodium salt and HA acid form as both materials were used as substrates for acylation reaction. For this reason, the obtained hyaluronan acid form was divided into two parts. One part of the material was used for acylation reaction in its acid form. The second half of hyaluronan acid form was returned into its initial sodium salt state in a following way. Hyaluronan acid form was diluted in water, neutralized to pH 6.5 and precipitated off with absolute 2-propanol. The precipitate was washed three times with 80% 2-propanol, twice with absolute 2-propanol and dried at 40 °C.

2.3. Acylation of hyaluronan sodium salt (Ac-HA-Na)

HA sodium salt (5 g) was first dissolved in 50 mL of demineralized water and then diluted with 50 mL of DMSO. Hexanoic anhydride (2.5 equiv./HA dimer), triethylamine (2.5 equiv./HA dimer) and DMAP (0.05 equiv./HA dimer) were added into the mixture and the mixture was stirred at room temperature for 2 h. At the end of reaction, the mixture was diluted with 100 mL of water followed by the addition of 15 mL of saturated NaCl solution. The product Ac-HA-Na (acylated HA-Na^+ in its Na^+ form) was precipitated with another 200 mL of absolute 2-propanol. The precipitate was first washed three times with 80% 2-propanol in water and then with absolute 2-propanol. The solid was filtered and dried in oven at 40 °C. The yield of final product was 5.4 g. The degree of substitution (DS) calculated from NMR spectra was 70%.

2.4. Acylation of hyaluronan acid form (Ac-HA-H)

Hyaluronan acid form (5 g) was dissolved in 100 mL of DMSO. Hexanoic anhydride (1.5–3.0 equiv./HA dimer), triethylamine (1.5, 2.5 and 3.0 equiv./HA dimer) and DMAP (0.05 equiv./HA dimer) were added into the mixture and the mixture was stirred at room temperature for 2 h. At the end of reaction, the reaction was quenched with 100 mL of water and the pH was adjusted with 0.1 M NaOH to pH 6, followed by the addition of 15 mL of saturated NaCl solution. The product Ac-HA-H (acylated HA-H^+ in its Na^+ form) was precipitated with 200 mL of absolute 2-propanol. The precipitate was washed three times with 80% 2-propanol in water and then absolute 2-propanol. The solid was filtered and dried in oven at 40 °C. The yield of final product was between 4.5 and 4.8 g. The degree of substitution (DS) calculated from NMR spectra was 33%, 60% and 70% for 1.5, 2.5 and 3.0 equiv. of triethylamine/HA dimer, respectively.

2.5. NMR analyses

HA acyl derivates (10 mg) were solubilized in 750 μL of D_2O, transferred into NMR tubes and directly analyzed.

The NMR analyses were performed on Bruker Avance™ 500 MHz equipped with BBFO plus probe. The ^1H and ^{13}C chemical shift were referenced to 3-trimethylsilylpropanoic acid sodium salt (TSPA) used as an internal standard. ^1H–^1H TOCSY spectra were recorded with 2048 data points, 80 scans per increment and 128 increments. TOCSY mixing time was set at 80 ms. ^1H–^{13}C HSQC spectra were acquired using gradient pulse sequences and 2048 data points, 80 scans per increment, 256 increments, and heteronuclear scalar coupling C–H set at 145 Hz. DOSY (diffusion ordered spectra) were obtained using a stimulated echo pulse sequence with bipolar gradients (STEBPGP). Scans (32) were collected using 2.5 ms sine-shaped pulses (5 ms bipolar pulse pair) ranging from 0.674 to 32.030 G cm^{-1} in 24 increments with a diffusion time of 200–600 ms, and 8192 time domain data points. Apodization was made by multiplying the data with a line broadening of 1.0 Hz, spike suppression factor of 4.0, maximum interactions number set to 100, noise sensitivity factor of 2, and number of components set to 1.

^1H NMR spectra were used for the calculation of the degree of substitution (DS) of acylated HA. DS (in %) was determined as relative integral of signal at 2.4 ppm, when the integration of signal at 2.0 ppm was normalized to 150. Explanation of resonating signals is given in the text.

2.6. MS analyses

Powdered hyaluronan (100 mg) was first dissolved in 10 mL of 0.1 M sodium acetate with 0.15 M NaCl (pH 5.3, adjusted with glacial acetic acid), and then incubated with 2000 IU of hyaluronidase (Finepharm) at 37 °C for 2 days. The enzyme was removed by short boiling of the solution at the end of incubation. The sample was filtered through 0.2 μm Nylon syringe filter. Filtered solution (2 mL) was transferred into the Vivaspin 15R concentrator (2000 MWCO Hydrosart, Sartorius) and centrifuged at 9000 rpm for 15 min. After preconcentration of the sample, the concentrator was filled with 10 mL of deionized water and centrifuged at 9000 rpm for 30 min. 4 wash cycles were used to remove the initial salt content. The sample was recovered from the bottom of the concentrator, diluted with 0.1% HCOOH:methanol = 1:1 to a final concentration of 1 mg mL^{-1} and directly injected into mass spectrometer.

Mass spectroscopic analyses of digested and desalted derivates were performed using a Synapt HDMS mass spectrometer (Waters), equipped with an electrospray ionization source operating in negative ion mode. The effluent was introduced into an electrospray source with a syringe pump at a flow rate of 10 μL min^{-1}. Nitrogen was used as cone gas (100 L h^{-1}) and desolvation gas (800 L h^{-1}). Capillary voltage was set at 3 kV. Sampling cone was set at 100 V. Extraction cone was set at 5 V. The source block temperature was set at 100 °C, while the desolvation temperature was 250 °C. For

each sample full MS and MS/MS scans from m/z 50 to 2000 were acquired for 2 min. For MS/MS measurements, argon was used as a collision gas. The collision energy was optimized to fragment the ion of interest, typically 55 eV for the ions with higher m/z and 25 eV for the ions with lower m/z. Data were collected at 1 scan s^{-1} and elaborated using MassLynx software.

2.7. UV–vis analyses

Powdered HA (10–200 mg) HA 34 kDa, HA 155 kDa, Ac-HA-H and Ac-HA-Na was first soaked with 750 μL of H_2O and then left dissolving overnight under constant stirring. Then 200 μL of Oil Red O solution (20 mg mL^{-1} in hexane) was added to the dissolved HA samples, the mixtures were heated up to 50 °C and shaken for 2 h at 50 °C, and for 2 days at room temperature. The experiments were repeated in two independent series, each consisting of replicate samples. Absorbances (522 nm) of the water phase were measured with UV-Vis Carry 100 (Varian).

2.8. Thermal analyses

HA samples of approximately 2 mg (weighted with an accuracy of ±0.01 mg) were placed in aluminum sample pans (TA Instruments, Tzero® Technology) and the excess of water (milli-Q) was added. Surplus of water was allowed to slowly evaporate at room temperature until the desired water content (W_c = mass of water (g)/mass of dry sample (g); [W_c] = g g^{-1}) was obtained. Several samples having W_c between 0.1 and 3 g g^{-1} were prepared for each HA material. The pans were subsequently hermetically sealed and left to equilibrate at room temperature for 72 h. Similar way of samples preparation was used for freezing/thawing as well as for the evaporation experiments.

Differential scanning calorimetry (DSC) was carried out using the TA Instruments DSC Q-200 equipped with a cooling accessory RCS-90 and assessed by the TA-Universal Analysis 2000 software.

The following thermal protocol was used for freezing/thawing experiments: start at 40.0 °C; cooling from 40.0 to −70.0 °C at 3.0 °C min^{-1}; isothermal at −70.0 °C for 1.0 min; heating from −70.0 to 40 °C at 5.0 °C min^{-1}. Flow rate of dynamic nitrogen atmosphere was 50 mL min^{-1}.

The following thermal protocol was used for the measurement of evaporation enthalpy: equilibration at 27.0 °C; cooling from 27.0 to −50.0 °C at 10.0 °C min^{-1}; isothermal at −50.0 °C for 1.0 min; heating from −50.0 to 200.0 °C at 5.0 °C min^{-1} and switching the flow rate of nitrogen from 50 mL min^{-1} to 5 mL min^{-1}. Immediately before the measurement, the hermetic lid (necessary for the sample preparation) was perforated using a sharp tool and the measurement was carried out straightway (Průšová, Šmejkalová, Chytil, Velebný, & Kučerík, 2010).

To obtain precise water content, thermogravimetry (TA Instruments, Q500 IR) was used to determine the equilibrium moisture content as a mass loss in the temperature interval 25–220 °C under dynamic atmosphere of nitrogen 25 mL min^{-1}.

2.9. Size exclusion chromatography coupled to multi-angle light scattering (SEC-MALS)

SEC was performed using an Agilent 1100 series liquid chromatograph equipped with a degasser (Model G1379A), an isocratic HPLC pump (Model G1310A), an automatic injector (Model G1313A), a column thermostat (Model G1316A), a DAWN EOS multi-angle light scattering photometer followed by an Optilab rEX differential refractometer (both from Wyatt Technology Corporation, USA). The injection volume was 100 μL of 0.1–1.0% (w/v) solutions. The separation was carried out using PL aquagel-OH 40 (300 mm × 7.5 mm; 8 μm) and PL aquagel-OH 20 (300 mm × 7.5 mm; 5 μm) columns connected in series. Columns were thermostated at 40 °C. The mobile phase was 0.1 M sodium phosphate buffer (pH adjusted to 7.5) + 0.05% NaN_3 at a flow rate 0.8 mL min^{-1}. Data acquisition and molecular weights calculations were performed using the ASTRA V software (Wyatt Technology Corporation, USA). The specific refractive index increment dn/dc was determined at 690 nm using the Optilab rEX refractometer for all samples according to procedure described elsewhere (Podzimek, Hermannová, Bílerová, Bezáková, & Velebný, 2010). The mean value of 9 dn/dc measurements was 0.155 ± 0.003 mL g^{-1}.

Each sample was filtered through Acrodisc Syringe Filter 0.45 μm 25 mm diameter with the Supor membrane (Pall). All reagents for SEC were HPLC grade and the mobile phase was filtered through Nylaflo Nylon Membrane Filter 0.2 μm (Pall).

3. Results and discussion

3.1. Acylation of hyaluronan

One of the main problems related to chemical modification of hyaluronan is its insolubility in organic solvents. For this reason, hyaluronan is mostly transformed prior modification into its acid form which is soluble in polar organic solvents such as DMSO (Oudshoorn, Rissmann, Bouwstra, & Hennink, 2007). However, the major disadvantage of this procedure is the contemporary degradation of HA during cation exchange step. For example, in this work a starting HA material was having M_w = 200 kDa, while after transformation into its acid form the M_w was reduced to about 50 kDa. For this reason, we tried to overcome this disadvantage by a direct acylation of hyaluronan as sodium salt in DMSO/H_2O solution. The acylation reactions are shown in Fig. 1. Regardless of the starting material and solvent choice, sodium salt of acylated HA was formed in both cases (Fig. 1). However, since the choice of reaction solvent may affect substitution position on HA chain, modified HA products received after acylation in DMSO (Ac-HA-H) and DMSO/H_2O (Ac-HA-Na) were further analyzed and compared by NMR, LC–MS, UV–vis and thermal analysis.

3.2. NMR analyses

^{1}H NMR spectra of HA, Ac-HA-H and Ac-HA-Na are shown in Fig. 2. All of the spectra show typical proton chemical shifts of HA involving signal at 2.0 ppm belonging to $COCH_3$ group, skeletal signals at 3.4–3.9 and anomeric resonances at 4.4–4.6 ppm. Remaining signals detected in modified HA at 0.8, 1.2, 1.5 and 2.4 ppm were attributed to the CH_2 in acyl chain as shown in Fig. 2. Relative integration of signals at 2.0 and 2.4 ppm were used for the determination of degree of substitution (DS). A comparable DS = 70% was determined for both acylated products shown in Fig. 2. A downfield chemical shift of one of the HA skeletal signals is evident in Ac-HA-Na at 3.1 ppm. Less significant is the appearance of a new signal at 3.3 ppm in Ac-HA-H. The new signals detected after HA modification are different for Ac-HA-Na and Ac-HA-H, and thus suggest that acylation reaction in DMSO yielded structurally different reaction outcome as compared to DMSO/H_2O reaction.

The linkage between hexyl chain and HA was established in both derivates by DOSY experiment (data not shown). Because of the marked difference between the diffusion coefficients of hexanoic acid and HA, the DOSY map can easily establish the presence of non-attached hexanoic acid to HA, which obviously is much faster than the diffusion of the bound acyl chain. In both cases, DOSY experiments showed similar diffusion behavior for all signals between 0.8 and 4.6 ppm (except for isopropanol and HDO signal) and thus indicated that all of the proton resonances in this region belonged to one structural complex.

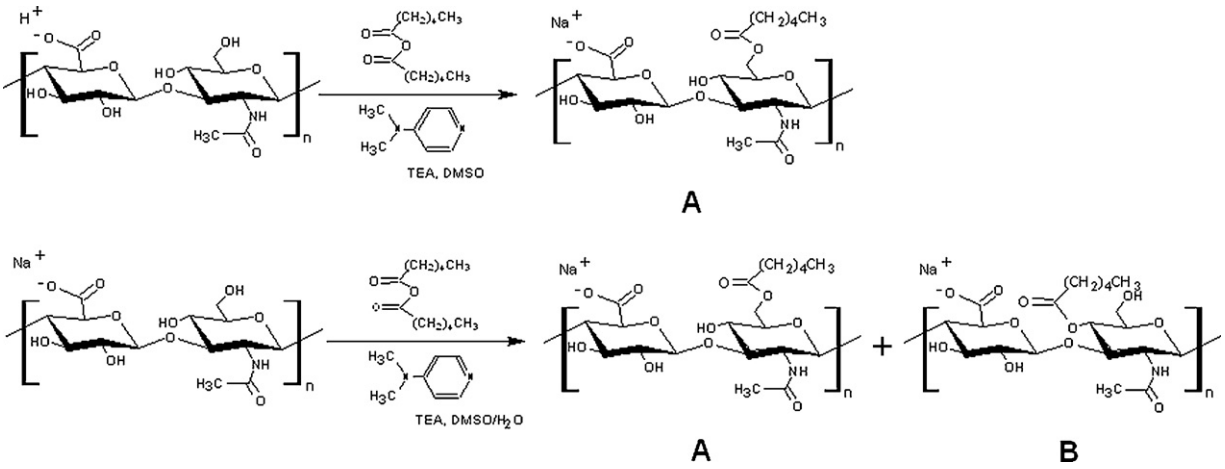

Fig. 1. Synthesis of Ac-HA-H (upper scheme) and Ac-HA-Na (lower scheme).

The structural diversity between Ac-HA-H and Ac-HA-Na was further evidenced in HSQC spectra (Fig. 3). These NMR spectra were detected in edited mode, enabling the recognition of CH and CH_3 signals (positive) from those of CH_2 (negative). The CH_2 group in HA possesses two protons that are diastereotopic (magnetically nonequivalent), and for this reason instead of one, there are two proton signals at 3.8 and 3.9 ppm correlating with one carbon shift (Fig. 3). Since there is only one CH_2 in HA it is easily recognizable in edited HSQC spectra of pure hyaluronan (spectrum not shown) as well as there is recognizable any chemical shift of this functional group resulting from the HA chemical modification in the close environment of the CH_2 group. Comparing HSQC spectra of Ac-HA-H and Ac-HA-Na there is in both cases a clear downfield shift of both C6 and H6, specific for the esterification of CH_2OH group in *N*-acetyl-D-glucosamine (product A in Fig. 1). In addition, in HSQC spectrum of Ac-HA-Na there is another shifted CH_2 correlation upfield to 3.6 and 3.7 ppm together with some extra downfield shifted CH crosspeaks in skeletal and anomeric region. The upfield shift of C6 in Ac-HA-Na may indicate esterification of OH group of *N*-acetyl-D-glucosamine in position 4 (product B in Fig. 1). Thus acylation in DMSO/H_2O is not as selective as that carried out only in DMSO.

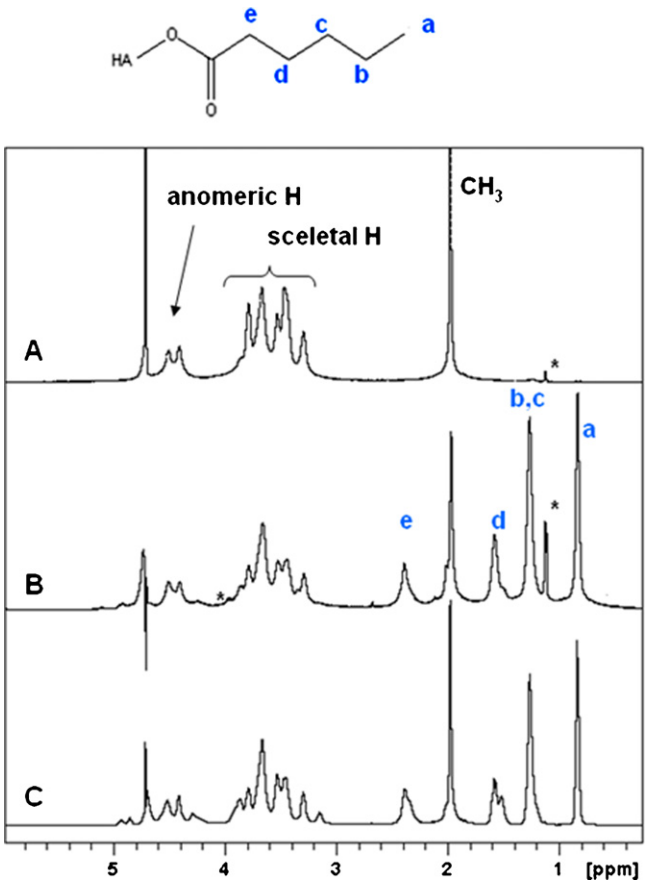

Fig. 2. ^1H NMR spectra of HA 155 kDa (A), Ac-HA-H (B), and Ac-HA-Na (C).

Lower reaction selectivity in DMSO/H_2O environment was also evidenced in TOCSY spectra (data not shown), where an extra spin system detected at 3.1–3.5–4.4 ppm was attributed to glucuronic acid belonging to the acylated HA in position 4 of *N*-acetyl-D-glucosamine (product B in Fig. 1). No such correlations were found for Ac-HA-H, where the reaction was carried out in DMSO only. Therefore, both products A and B (Fig. 1) were formed when acylation was carried out in DMSO/H_2O while product A (Fig. 1) was received as the major product when the same reaction was performed in DMSO.

3.3. MS analyses

ESI-MS and ESI-MS/MS analyses were carried out in order to confirm the structural differences between Ac-HA-H and Ac-HA-Na previously suggested from NMR spectra. ESI-MS spectra of both acylated products with DS = 70% after enzymatic degradation are reported in Fig. 4. There is no significant difference between the two spectra (Fig. 4), suggesting that the number of acyl chains per dimer unit in HA was comparable in both solvents. The spectra indicated the presence of unmodified HA dimer (m/z = 396), HA tetramer (m/z = 775), HA hexamer (m/z = 1154), HA octamer (m/z = 1533), and modified HA mers with one or two acyl chains (m/z is increased by 98 or 196, respectively) in case of HA tetramer and hexamer, three acyl chains (m/z is increased by 294) in case of HA hexamer and octamer, and four acyl chains (m/z is increased by 392) in case of HA octamer.

To compare the way of substitution, MS/MS spectra were collected for the most intensive peaks detected in ESI-MS spectra. The fragmentation pattern of both acylated products is similar and includes ions corresponding to the loss of acyl chain, glucuronic acid, and *N*-acetyl-D-glucosamine (Fig. 5). However, a clear difference may be noticed in the intensity of m/z = 291, corresponding to the modified glucuronic acid with hexyl chain. Being this intensity about 20% in Ac-HA-H sample, while less than 5% in Ac-HA-Na, there is hardly any modification of any OH group of glucuronic acid

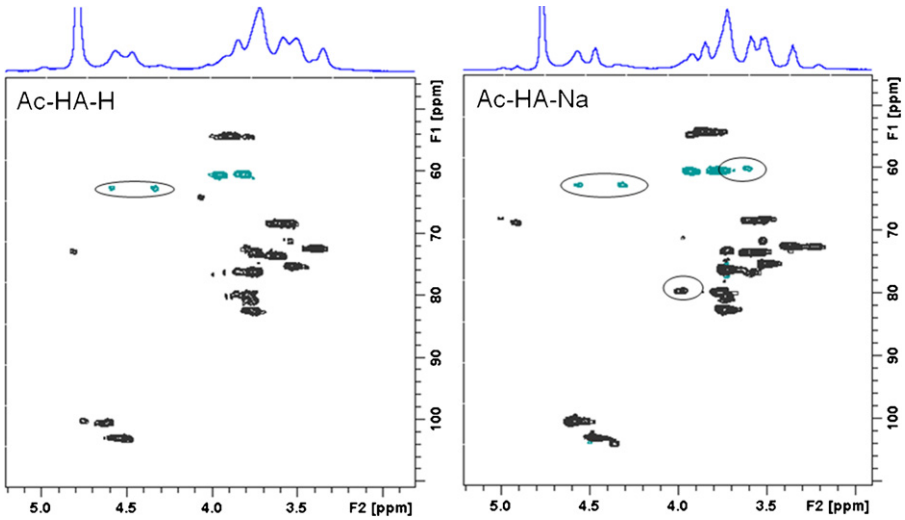

Fig. 3. 2D HSQC NMR spectra of Ac-HA-H and Ac-HA-Na. Structural differences are indicated by circles.

in Ac-HA-Na. This finding which was observed in all other MS/MS spectra (not shown), confirms the previous interpretation of NMR data, where the mixture of products A and B (Fig. 1) substituted with acyl chain in different positions on *N*-acetyl-D-glucosamine were suggested as the major products in DMSO/H_2O. Although product A was suggested as the major product in the case of Ac-HA-H, according to the results from MS spectra, acyl substitution of glucuronic acid cannot be excluded.

3.4. UV–vis analyses

In order to determine a possible hydrophobic aggregation of acyl chains in HA derivates, Ac-HA-H (DS from 33 to 70%) and Ac-HA-Na (DS = 70%) were mixed with Oil Red O which is a hydrophobic dye commonly used for staining of neutral triglycerides and lipids on froze sections and some lipoproteins on paraffin sections. Therefore, it is expected that Oil Red O will dissolve only in hydrophobic domains of HA. The results of Oil Red O absorption by two different HA concentrations are reported in Fig. 6. The lowest absorbance $A = 0.06–0.08$ of hydrophobic dye at hyaluronan concentration $c = 10\ mg\ mL^{-1}$ was observed for unmodified 34 kDa and acylated Ac-HA-H with DS = 33%, followed by unmodified HA 155 kDa ($A = 0.1$). Thus low degree of acylation did not induce any significant formation of hydrophobic domains. This situation changes for acylation degree of 60 and 70%, where the presence of hydrophobic domains is indicated by a 3.5 times higher absorbance ($A = 0.5$) as compared to control unmodified samples. In fact, in this case it seems that higher DS indicates larger amounts of hydrophobic domains in HA samples and for this reason also higher affinity towards hydrophobic compounds.

However, a completely different absorption behavior was observed at hyaluronan concentration $c = 15\ mg\ mL^{-1}$. Here, again the lowest absorbances ($A = 0.1–0.2$) were measured for HA 34 kDa and Ac-HA-H (DS = 33%). But then unlike the previous case, HA 155 kDa showed a two fold absorbance increase to $A = 0.4$, which was comparable to $A = 0.4$ and 0.5 observed for acylated samples Ac-HA-H with DS of 60 and 70%. The detected absorbance increase in 155 kDa HA is in agreement with the observation of hydrophobic patches in aggregated HA (Scott, Cummings, Brass, & Chen, 1991; Scott et al., 1990). No such observation was made in case of 34 kDa HA probably due to its lower molecular size. A significant change was found for Ac-HA-Na (DS = 70%) sample whose absorbance is a double from that of Ac-HA-H (DS = 70%). Since DS of the acylated HA in this last case is comparable, the amount of acyl chains attached to HA is not the only driving force influencing the amount of bound hydrophobic dye. The data suggest that except for DS, it is also important which OH group in HA is substituted. In Ac-HA-Na acylation mainly occurred either at position 4 or 6 of *N*-acetyl-D-glucosamine, while in Ac-HA-H in position 6. The absorption data suggest a more significant aggregation of acyl chains in Ac-HA-Na, which could have resulted from the vicinity of acyl chains within Ac-HA-Na secondary structure and easier formation of 'micelle-like' conformation as compared to Ac-HA-H. True micelles are not of course expected to form. Such conformation, however, seems to be concentration dependent.

3.5. Thermal analysis

Recent study has shown that methods of thermal analysis are useful in the determination of hyaluronan conformation by

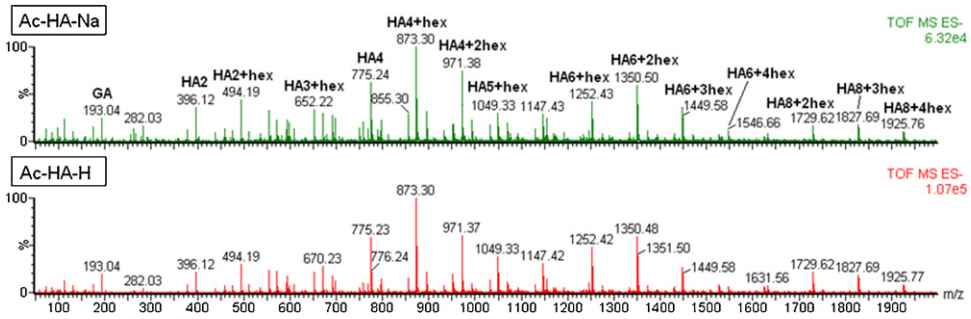

Fig. 4. ESI-MS spectra of Ac-HA-H and Ac-HA-Na after enzymatic degradation. HA2–HA8 stands for dimer–octamer of HA, GA for glucuronic acid and hex for hexyl chain.

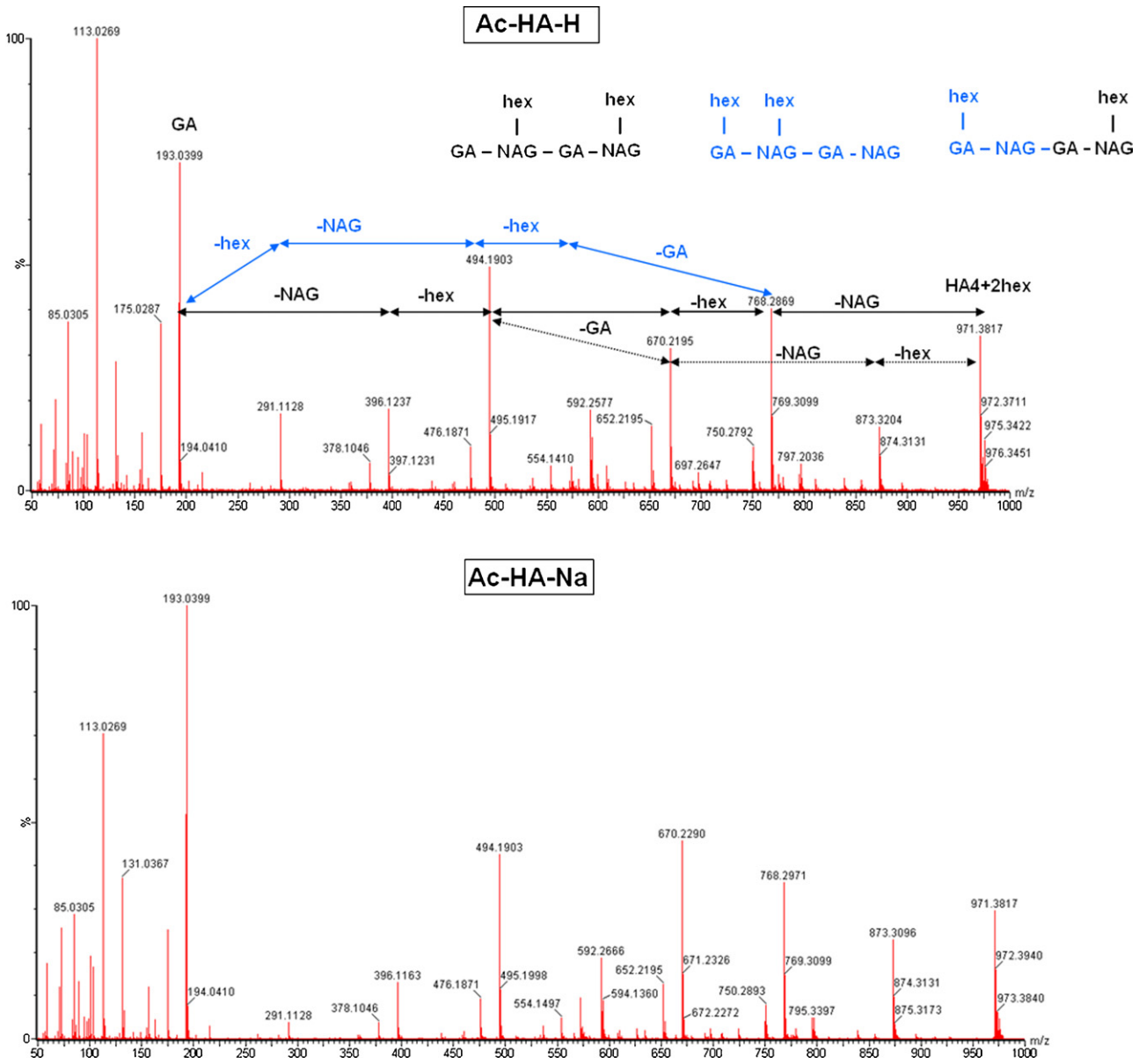

Fig. 5. MS/MS fragmentation (sampling cone set at 40 V) of m/z = 971 of Ac-HA-H and Ac-HA-Na with designed possible fragmentation pathways corresponding to the three indicated structures. NAG stands for *N*-acetyl-D-glucosamine, GA for glucuronic acid and hex for hexyl chain.

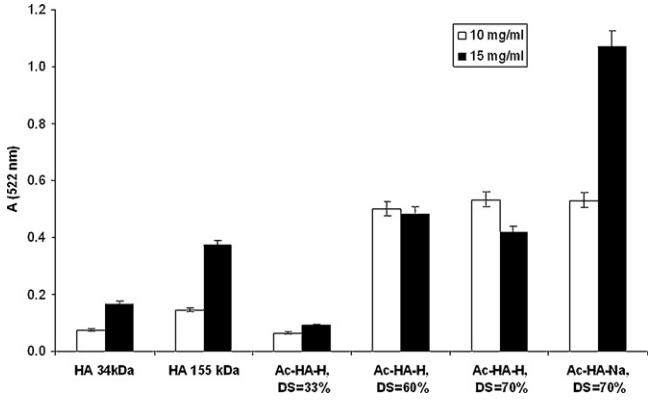

Fig. 6. Oil Red O absorption by HA and acylated HA with different degree of substitution (DS).

comparing hyaluronan hydration (Průšová et al., 2010). In this study we have repeated similar hydration experiments, namely water evaporation and melting. There were no obvious differences between hydration numbers of HA derivatives obtained from water evaporation experiments (data not shown). A clear difference was evidenced when comparing hydration data from classical melting experiments. It implies differences in the physical structure of dry derivatives and original hyaluronan. In principle, hydration numbers obtained from evaporation experiments reflect the state of structure in which a minimum of water molecules are present and strong interactions among hyaluronan segments take part (Průšová et al., 2010). Such number indicates solely the starting concentration but not the mechanisms of drying process itself. The derivatization causes small changes in flexibility and spatial arrangement of modified segments causing anomalies in physical structure of derivatives after drying. This was reflected mainly as differences in water vaporization enthalpies in individual samples (results no shown). In contrast, melting experiments provide hydration numbers indicating the state of (still preserved) physical

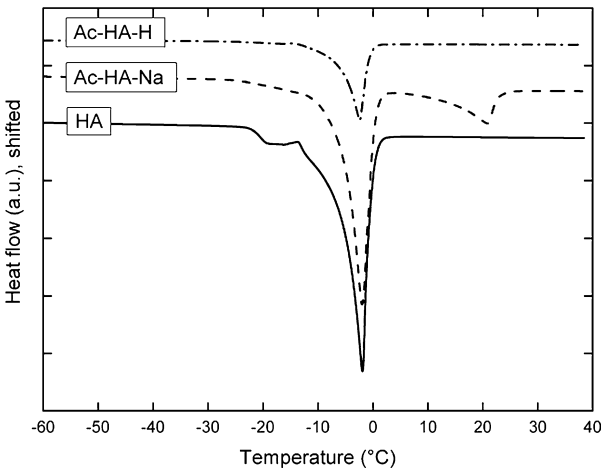

Fig. 7. Comparison of ice melting in native and acylated HA.

structure of dry hyaluronan covered by the monomolecular water layer. Therefore, using this approach the difference in pore size distribution and different surface wettability can be much better visualized. The DSC melting curves of ice present in acylated samples are shown in Fig. 7. As it can be seen, the melting behavior of Ac-HA-Na significantly differed from that of HA and Ac-HA-H. The main difference was in the detection of the second melting peak in Ac-HA-Na in the temperature range from 0 to 25 °C (Fig. 7). This peak was observable regardless the amount of water content in sample and its presence was confirmed on crystallization curve (data not shown). The detection of two distinguishable peaks on DSC curves (Fig. 7) indicates, that there exist two possible way of water binding in Ac-HA-Na sample reflected by two different crystallization/melting mechanisms. The first type of water binding resembles the hydration of ordinary structure of HA. Second type of water binding detected only in Ac-HA-Na derivates cannot be associated with hydration of ordinary HA structure and shows different hydration behavior, which is most probably associated with the presence of confined water. Confined water can be found in granular and porous materials and around and within macromolecules and gels (Chaplin, 2010). Physical properties and state of that water may vary widely depending on the molecular characteristics of the cavity surface and the confinement dimensions, as well as temperature and pressure. The properties of the confined water are difficult to predict and may be very different from those of bulk water which is particularly true when the confinement is on the nano-scale level (Chaplin, 2010). For example surface interactions and the confinement diameter may cause that the ice is formed at 400 K in very narrow pores (0.6–1.0 nm diameter) in porous glass (Venzel, Egorov, Zhizhenkov, & Kleiner, 1985). In accordance with literature, we hypothesize, that Ac-HA-Na sample contains cavity with both hydrophilic and hydrophobic surface. The cavity size and wettability influences the physical properties of encapsulated water which in turn causes anomaly high melting temperature of formed ice.

4. Conclusion

In summary, HA acylation in DMSO and DMSO/H_2O yields structurally different products which were elucidated by means of NMR, MS, DSC and UV/vis. Acylation reaction carried out in DMSO (Ac-HA-H) was more selective as compared to that performed in DMSO/H_2O (Ac-HA-Na). NMR analyses indicated that Ac-HA-H was preferentially substituted in position 6 of *N*-acetyl-D-glucosamine, while either position 6 or 4 of *N*-acetyl-D-glucosamine unit were acylated in Ac-HA-Na. Mass analyses detected that in average there is a maximum of 1 acyl chain per HA dimer unit for both types of acylated products. However, due to the different positions of functionalization in HA structure, DSC and UV/vis analyses revealed different conformational and hydration behavior of the two derivates. For concentrated samples, the formation of hydrophobic domains was inevitably detected in the solution of Ac-HA-Na. These results are useful for developing biomedical application of this biomaterial as drug carrier.

Acknowledgement

AP and JK thank the Ministry of Education, Youth and Sport of the Czech Republic project no. 0021630501.

References

Abatangelo, G., Barbucci, R., Brun, P. & Lamponi, S. (1997). Biocompatibility and enzymatic degradation studies on sulphated hyaluronic acid derivates. *Biomaterials*, *18*, 1411–1415.

Akiyoshi, K. & Sunamoto, J. (1996). Supramolecular assembly of hydrophobized polysaccharides. *Supramolecular Science*, *3*, 157–163.

Chaplin, M. F. (2010). Structuring and behaviour of water in nanochannels and confined spaces. In L. J. Dunne, & G. Manos (Eds.), *Adsorption and phase behaviour in nanochannels and nanotubes* (pp. 241–256). Netherlands: Springer.

Collis, L., Hall, C., Lange, L., Ziebell, M., Prestwich, R. & Turley, E. A. (1998). Rapid hyaluronan uptake is associated with enhanced mobility: Implications for an intracellular mode of action. *FEBS Letters*, *440*, 444–449.

Deleu, M. & Paquot, M. (2004). From renewable vegetables to microorganisms: New trends in surfactants. *Comptes Rendus Chimie*, *7*, 641–646.

Entwistle, J., Hall, C. L. & Turley, E. A. (1996). HA receptors: Regulators of signaling to the cytoskeleton. *Journal of Cellular Biochemistry*, *61*, 569–577.

Hill, K. & LeHen-Ferrenbach, C. (2008). Sugar-based surfactants for consumer products and technical applications. In C. C. Ruiz (Ed.), *Sugar based surfactants. Fundamentals and applications* (pp. 1–20). New York: CRC Press.

Kawaguchi, Z., Matsukawa, K. & Ishigami, Y. (1993). Conformational changes of hyaluronates with partial palmitoylation and the adsorption structures on the surface of oil droplets. *Carbohydrate Polymers*, *20*, 183–187.

Kong, M., Chen, X. & Park, H. (2011). Design and investigation of nanoemulsified carrier based on amphiphile-modified hyaluronic acid. *Carbohydrate Polymers*, *83*, 462–469.

Laurent, T. C. (1998). *The chemistry, biology and medical applications of hyaluronan and its derivates*. London: Portland Press.

Oh, E. J., Park, K., Kim, K. S., Kim, J., Yang, J.-A., Kong, J.-H., et al. (2010). Target specific and long-acting delivery of protein, peptide, and nucleotide therapeutics using hyaluronic acid derivates. *Journal of Controlled Release*, *141*, 2–12.

Oudshoorn, M. H. M., Rissmann, R., Bouwstra, J. A. & Hennink, W. E. (2007). Synthesis of methacrylated hyaluronic acid with tailored degree of substitution. *Polymer*, *48*, 1915–1920.

Podzimek, S., Hermannová, M., Bílerová, H., Bezáková, Z. & Velebný, V. (2010). Solution properties of hyaluronic acid and comparison of SEC-MALS–VIS data with off-line capillary viscometry. *Journal of Applied Polymer Science*, *116*, 3013–3020.

Prestwitch, G. D., Marecak, D. M., Marecek, J. F., Vercruysse, K. P. & Ziebell, M. R. (1998). Controlled chemical modification of hyaluronic acid: Synthesis, applications, and biodegradation of hydrazide derivates. *Journal of Controlled Release*, *53*, 93–103.

Prestwitch, G. D. & Vercruysse, K. P. (1998). Profiles therapeutic applications of hyaluronic acid and hyaluronan derivates. *Pharmaceutical Science & Technology Today*, *1*, 42–43.

Průšová, A., Šmejkalová, D., Chytil, M., Velebný, V. & Kučerík, J. (2010). An alternative approach to study hydration of hyaluronan. *Carbohydrate Polymers*, *82*, 498–503.

Scott, J. E. (1998). Chemical morphology of hyaluronan. In T. C. Laurent (Ed.), *The chemistry, biology and medical applications of hyaluronan and its derivates* (pp. 7–15). London: Portland Press.

Scott, J. E., Cummings, C., Brass, A. & Chen, Y. (1991). Secondary and tertiary structures of hyaluronan in aqueous solution, investigated by rotary shadowing-electron microscopy and computer simulation. Hyaluronan is a very efficient network-forming polymer. *Biochemical Journal*, *274*, 699–705.

Scott, J. E., Cummings, C., Greiling, H., Stuhlsatz, H. W., Gregory, J. D. & Damle, S. P. (1990). Examination of corneal proteoglycans and glycosaminoglycans by rotary shadowing and electron microscopy. *International Journal of Biological Macromolecules*, *12*, 180–184.

Šoltés, L., Mendichi, R., Kogan, G., Schiller, J., Stankovská, M. & Arnhold, J. (2006). Degradative action of reactive oxygen species on hyaluronan. *Biomacromolecules*, *7*, 659–668.

Taglienti, A., Valentini, M., Sequi, P. & Crescenzi, V. (2005). Characterization of methylprednisolone esters of hyaluronan in aqueous solution: Conformation and aggregation behavior. *Biomacromolecules*, *6*(3), 1648–1653.

Venzel, B. I., Egorov, E. A., Zhizhenkov, V. V. & Kleiner, V. D. (1985). Determination of the melting point of ice in porous glass in relation to the size of the pores. *Journal of Engineering Physics and Thermophysics*, *48*, 346–350.